Available online at www.sciencedirect.com
ScienceDirect
Mathematics and Computers in Simulation 214 (2023) 133–151
MATHEMATICS AND COMPUTERS IN SIMULATION
www.elsevier.com/locate/matcom

Original articles

Analysis of nonlinear compartmental model using a reliable method

Juan Luis García Guirao[a,*], Mansoor Alsulami[b], Haci Mehmet Baskonus[c], Esin Ilhan[d], P. Veeresha[e]

[a] *Departamento de Matematica Aplicada y Estadistica, Universidad Politecnica de Cartagena, Hospital de Marina, Murcia, 30203, Spain*
[b] *Mathematical Modeling and Applied Computation Research Group (MMAC), Department of Mathematics, King Abdulaziz University, P.O. Box 80203, Jeddah 21589 Saudi Arabia*
[c] *Department of Mathematics and Science Education, Faculty of Education, Harran University, Sanliurfa, Turkey*
[d] *Faculty of Engineering and Architecture, Kirsehir Ahi Evran University, 40500 Kirsehir, Turkey*
[e] *Center for Mathematical Needs, Department of Mathematics, CHRIST (Deemed to be University), Bengaluru 560029, India*

Received 13 April 2023; received in revised form 5 June 2023; accepted 2 July 2023
Available online 13 July 2023

Abstract

The goal of this work is to investigate nonlinear models and their complexity using techniques that are universal and have connections to historical and material aspects. Using the premise of a constant population that is uniformly mixed, a nonlinear compartmental model that depicts the movement between voter classes is taken into consideration. In the current work, we investigate the dynamical framework that supports the interactions between the three parties. It is discussed how rate change affects various metrics. The conditions for boundedness, stability, existence, and other dynamics are obtained. We derive the effects of generalizing the model in any order. The current study supports investigations into complex real-world issues and forecasts of necessary plans.

Keywords: Caputo fractional derivative; Numerical method; Chaotic behaviors; Political parties

1. Introduction

Mathematical modeling and numerical methods are the best tools for investigating complex problems in physics, chemistry [31], and biology. In particular, analyzing phenomena based on complex combinations is a highly magnetized area of research where many young researchers are inclined towards research where they can derive the most stimulating behaviors using suitable mathematical software. Recently we can notice the number of research articles available in the literature to illustrate the essence and impact of differential equations, particularly ordinary differential equations which seem simple but depend on one independent variable; they can only offer a highly complex nature including chaotic behavior. Researchers have worked to understand this fascinating nature of dynamical systems with chaotic behavior since Lorentz first observed such behavior in electron interactions. These systems, which exhibit the butterfly effect and asymptotic stability, are interesting for researchers. However, this

* Corresponding author.
E-mail addresses: juan.garcia@upct.es (J.L.G. Guirao), maalsulami2@kau.edu.sa (M. Alsulami), hmbaskonus@harran.edu.tr (H.M. Baskonus), eilhan@ahievran.edu.tr (E. Ilhan), pundikala.veeresha@christuniversity.in (P. Veeresha).

https://doi.org/10.1016/j.matcom.2023.07.001

interest has also prompted the creation of many tools that help analyze these models efficiently. The significance of modeling in advanced manufacturing technology implementation is investigated [12] and discrete time queueing-inventory model is examined with back-order of items by researchers in [2]. Further, predictor–corrector method is effectively used in [23] to investigate about the SIR model with 2019-nCoV.

Recently, we witnessed many interesting results published within the frame of mathematical models associated with many diverse areas. For instance, the seismic resilience evaluation of the water supply system is examined in [43], the children's cognitive function and mental health are modeled in [32], the school student's academic performance during Covid-19 is natured using machine learning in [47], the complex Ginzburg–Landau equation is numerically analyzed in comparison with results available in the literature by researchers in [53], the implementation in small and medium-sized enterprises are effectively analyzed in [13], the special case of Korteweg–De Vries equation on critical flow over a hole is effectively and graphically examined using three fractional operators in [51]. These studies help and motivate us to conduct the present work.

Nature's complexity has long attracted researchers to complicated model patterns. Another instance of it is when none of its properties can be accurately represented by any formalization. Mathematically modeling a political system with three parties is important because it provides a mathematical framework for analyzing the behavior of the parties and the outcomes of elections. This allows us to better understand the dynamics of the political system, predict future outcomes, and potentially identify ways to improve the system. There are several reasons why mathematical modeling of a political system with three parties is necessary. First, it allows us to quantify the impact of different factors on election outcomes, such as voter preferences, party ideology, campaign spending, and other variables. Second, it may help identify trends or patterns that are difficult to observe through qualitative analysis alone. Finally, mathematical modeling allows for the testing of different scenarios and hypothetical situations in a way that is not possible through empirical research alone. Modeling the dynamics of the political parties with reliable assumptions is an important investigation for analyzing and improving political systems, and can help us better understand the behavior of politicians and voters in complex electoral systems. For every individual who enters the system, a different person exits it. In the majority of nations, citizens who turn 18 years or immigrants who obtain citizenship join the group of people who are eligible to vote. It is expected that interacting with a party member and the likelihood of acquiring their ideology will have an impact on the decision an eligible voter makes.

In the present investigation, we assumed the total population N remains constant [5]. Let P_A, P_B and P_C be three political parties with per capita recruitment rate α_1, α_2 and α_3, respectively. The difference between the per capita recruitment rate of P_B from party P_A and P_A from party P_B is symbolized as Ω_1. In the same manner, Ω_2 is the recruitment rate of P_C from party P_B and P_B from party P_C, and Ω_3 is the recruitment rate of P_A from party P_C and P_C from party P_A. The individuals enter and leave the voting system rate is denoted as β. The dynamics is presented as follows

$$\begin{aligned}
\frac{dP_A}{dt} &= P_A[\alpha_1(1 - P_A - P_B - P_C) + \Omega_3 P_C - \Omega_1 P_B - \beta],\\
\frac{dP_B}{dt} &= P_B[\alpha_2(1 - P_A - P_B - P_C) + \Omega_1 P_A - \Omega_1 P_C - \beta],\\
\frac{dP_C}{dt} &= P_C[\alpha_3(1 - P_A - P_B - P_C) + \Omega_2 P_B - \Omega_1 P_A - \beta].
\end{aligned} \tag{1}$$

Humanity chose the best instruments to study and record the ensuing effects in order to construct an ideal and successful mathematical model of the phenomena related to complicated nature. Despite the fact that calculus theory has been demonstrated to be the most accurate and efficient method for investigating and analyzing these phenomena using both differential and integral operators, many researchers during the twentieth century highlighted the associated system's limitations and the need to generalize it to include more significant physical properties related to history, time, material, and hereditary based properties. Many academics have recently been interested in fractional calculus (FC), which dates back to 1695, as a result of their inquisitive thinking [30,45].

Scientifically, fractional calculus provides a more realistic explanation of non-linear, non-local, and memory-dependent behavior in physical systems, which allows standard real-world models to be generalized to fractional order models [48,50]. Traditional models based on integer-order differential equations make the error of assuming that the process under consideration is instantaneous and memory-free, which is typically not the case in actuality. Fractional calculus provides a mathematical framework for describing systems with memory, non-locality, and non-linearity. Many domains, including signal processing, control engineering, and biomedical systems, have effectively

embraced fractional order models where standard integer order models are unable to accurately represent the system's behavior.

Numerous academics have noted that fractional calculus (FC) is a theoretical field that contributes little to innovation and is associated with difficult theoretical submission. The generalized dynamical model of cholera is proposed in [6], and the human liver is analyzed in [8] using Caputo–Fabrizio fractional derivative. The accelerated mass–spring system is effectively analyzed [18] using the fractional derivative, and we can find many interesting results derived with the help of fractional calculus [25,44]. However, the idea of fractional calculus has undergone a significant transformation as a result of Michele Caputo's technique from 1967 cite [15]. Despite the fact that most of them think the tool's limitations are mostly caused by current constraints [16,37,41]. Now, both for integral and differential operators, we provide a number of notions. The bulk of the newly proposed notations, however, can only be generalized with the help of the Caputo operator. Additionally, some researchers study alternative models in relation to this operator cite [3,17]. The evaluation of new fractional operators Ref. [7,27] and the old ones led to the careers of several young academics [4,10,34,49].

In this paper, we analyze the Adams–Bashforth-Moulton (ABM) technique, a well-posed numerical scheme [9, 19,28]. Many scholars use the same approach for complicated models even when they are described in terms of partial differential equations by transforming them into ODEs since the proposed strategy is particularly effective in studying the ODEs [1,20,21]. Eq. (1) is used to help us consider the fractional model in this instance

$$\begin{aligned} D_t^{\rho} P_A(t) &= P_A[\alpha_1(1 - P_A - P_B - P_C) + \Omega_3 P_C - \Omega_1 P_B - \beta], \\ D_t^{\rho} P_B(t) &= P_B[\alpha_2(1 - P_A - P_B - P_C) + \Omega_1 P_A - \Omega_2 P_C - \beta], \\ D_t^{\rho} P_C(t) &= P_C[\alpha_3(1 - P_A - P_B - P_C) + \Omega_2 P_B - \Omega_3 P_A - \beta]. \end{aligned} \tag{2}$$

Here, ρ is the fractional order. The spread of two political parties is mathematically modeled in [38], and then it was extended by the presence of switching [39]. Further, the dynamics of the poaching from one party to another is investigated in [33]. The potential margin of vague state voters for a particular party is mathematically modeled by researchers in [11]. The significance of the decline of class in democratic politics is theoretically investigated in [24], and the stability of the dynamical system of the multiparty political system is derived in [40]. The researchers in [22] investigated voting in multiparty elections with a model approach and derived strategic voting with the condition for constituency context. Later, the dynamics of voters and three political parties are mathematically analyzed by researchers [9,14], and the chaotic behavior in terms of Hopf bifurcation is captured in [26]. These studies encourage us to use effective numerical methods to demonstrate the system chaotic nature. However, we have not find the generalized model with the help of a novel fractional operator.

2. Basic results

Theorems and findings used to examine the system's stability and boundedness are presented in this section.

Definition 2.1 (*[42]*)**.** The Caputo fractional derivative with order ρ for $'n'$ times continuously differentiable function $f(t)$ is given by

$${}_{t_0}^{C}D_t^{\rho} f(t) = \frac{1}{\Gamma(n-\rho)} \int_{t_0}^{t} \frac{f^{(k)}(\varsigma)}{(t-\varsigma)^{\rho+1-n}} d\varsigma, n-1 < \rho < n, \tag{3}$$

where the Gamma function is denoted by $\Gamma(\cdot)$.

Definition 2.2 (*[36]*)**.** If $|arg(\lambda(A))| > \frac{\rho\pi}{2}$, the autonomous system $D^{\rho}x(t) = Ax(t), x(0) = x_0$ is asymptotically stable. If and only if the critical eigenvalues that meet the condition $|arg(\lambda(A))| = \frac{\rho\pi}{2}$ have geometric multiplicity 1, the system is said to be stable. The argument of the eigenvalues of the square matrix A is indicated here by the symbol $arg(\lambda(A))$.

Lemma 2.3 (*[52]*)**.** *For the system*

$${}_{t_0}^{C}D_t^{\rho} y(t) = g(t, y), t > t_0, \tag{4}$$

with the initial condition $y(t_0)$, where $0 < \rho \leq 1$ and $g : [t_0, \infty] \times \Psi \to \mathbb{R}^n$, $\Psi \in \mathbb{R}^n$. There exists only one solution of Eq. (4) on $[t_0, \infty) \times \Psi$ if the local Lipschitz condition with respect to y is followed by $g(t, x)$.

Lemma 2.4 (*[29]*). *Let $g(t)$ be a continuous function on $[t_0, +\infty)$ and satisfying*

$$ {}^{C}_{t_0}D^{\rho}_{t} g(t) \leq -\psi g(t) + \nu, g(t_0) = g(t_0). \tag{5} $$

Here, $0 < \rho < 1$, $(\psi, \nu) \in \mathbb{R}^2$, $\psi \neq 0$ and $t_0 \geq 0$ is the initial time. Then

$$ g(t) \leq \left(g(t_0) - \frac{\nu}{\psi} \right) E_{\rho}[-\psi (t - t_0)^{\rho}] + \frac{\nu}{\psi}. \tag{6} $$

Lemma 2.5 (*[35]*). *The equilibrium y_0 is globally stable if a function $G(y)$ is globally positively definite, radially unbounded, and its time derivative is globally negative, $G'(y) < 0$ for all $y \neq y_0$.*

3. Boundedness

The boundedness of the solutions of Eq. (2) is established as follows:

Theorem 3.1. *The solutions of the projected model (2) are uniformly bounded.*

Proof. Let $\mathcal{M}(t) = P_A(t) + P_B(t) + P_C(t)$. By considering the fractional derivative, one can get

$$ \begin{aligned} {}^{C}_{t_0}D^{\rho}_{t} \mathcal{M}(t) + \hbar_1(t) &= {}^{C}_{t_0}D^{\rho}_{t} [P_A(t) + P_B(t) + P_C(t)] + \hbar_1(t)[P_A(t) + P_B(t) + P_C(t)] \\ &= P_A[\alpha_1(1 - P_A - P_B - P_C) + \Omega_3 P_C - \Omega_1 P_B - \beta] \\ &\quad + P_B[\alpha_2(1 - P_A - P_B - P_C) + \Omega_1 P_A - \Omega_2 P_C - \beta] \\ &\quad + P_C[\alpha_3(1 - P_A - P_B - P_C) + \Omega_2 P_B - \Omega_3 P_A - \beta] + \hbar_1(t)[P_A(t) + P_B(t) + P_C(t)] \\ &\leq P_A(\alpha_1 + \Omega_3 P_C) + P_B(\alpha_2 + \Omega_1 P_A) + P_C(\alpha_3 + \Omega_2 P_B) + \hbar_1(t)[P_A(t) + P_B(t) + P_C(t)]. \end{aligned} \tag{7} $$

The solution exists and is unique in

$$ \Lambda = \{(P_A, P_B, P_C) : max\{(P_A|, (P_B|, (P_C|\} \leq \mathcal{N}\}. \tag{8} $$

The above inequality yields,

$$ {}^{C}_{t_0}D^{\rho}_{t} \mathcal{M}(t) + \hbar_1(t) \leq + \left(\frac{(\eta + 1)}{\alpha} + 1 + \frac{f}{\beta} + 3\hbar_1(t) \right) \mathcal{N}. $$

By Lemma 2.4, we get

$$ {}^{C}_{t_0}D^{\rho}_{t} \mathcal{M}(t) \leq \left(\mathcal{M}(t_0) - \frac{1}{\hbar_1(t)} ((\alpha_1 + \Omega_3 P_C) + (\alpha_2 + \Omega_1 P_A) + (\alpha_3 + \Omega_2 P_B) + 3\hbar_1(t)) \mathcal{N} \right) E_{\rho}(-\theta (t - t_0)^{\rho}) \tag{9} $$

$$ {}^{C}_{t_0}D^{\rho}_{t} \mathcal{M}(t) \to ((\alpha_1 + \Omega_3 P_C) + (\alpha_2 + \Omega_1 P_A) + (\alpha_3 + \Omega_2 P_B) + 3\hbar_1(t)) \mathcal{N}, t \to \infty. \tag{10} $$

Clearly, all the solutions of Eq. (2) that initiate in Λ remained bounded in

$$ \Xi = \{(P_A, P_B, P_C) \in \Lambda | N(t) \leq ((\alpha_1 + \Omega_3 P_C) + (\alpha_2 + \Omega_1 P_A) + (\alpha_3 + \Omega_2 P_B) + 3\hbar_1(t)) \mathcal{N} + \epsilon, \epsilon > 0\}. \quad \square $$

4. Stability of the equilibrium points

The signs of the eigenvalues of the linearization of the equations concerning the equilibria can be used to classify equilibria. The equilibrium point is hyperbolic if none of the eigenvalues have a real component with real value zero. If all of the eigenvalues have negative real parts, the point is stable. If at least one has a positive real component, the point is unstable. If at least one eigenvalue has a negative real portion and at least one has a positive real part, the equilibrium is a saddle point and unstable. If all of a point's eigenvalues are real and have the same sign, the point is referred to as a node.

The analysis of the stability of the equilibrium points using the Matignon criterion [46] is carried out in this section. In Fractional calculus, the study of stability is important to analyze the system's behavior which can also

be validated with the numerical approach. When the system behaves chaotically, it is argued that all equilibrium points are unstable. For the system (2), the Jacobian matrix of the system is given by

$$J = \begin{pmatrix} -\beta - \alpha_1 P_A + \alpha_1 \mathcal{K} - P_B \Omega_1 + P_C \Omega_3 & P_A(-\alpha_1 - \Omega_1) & P_A(\Omega_3 - \alpha_1) \\ P_B(\Omega_1 - \alpha_2) & -\beta + \alpha_2 \mathcal{K} + P_A \Omega_1 - \alpha_2 P_B - P_C \Omega_2 & P_B(-\alpha_2 - \Omega_2) \\ P_C(-\alpha_3 - \Omega_3) & P_C(\Omega_2 - \alpha_3) & -\beta + \alpha_3 \mathcal{K} - P_A \Omega_3 + P_B \Omega_2 - \alpha_3 P_C \end{pmatrix},$$

where $\mathcal{K} = (-u - v - w + 1)$. The equilibrium points of the system (2) are

$$E_1 = (-9.99001, 0.99001, 0), \quad E_2 = (0, 0, 0), \quad E_3 = (0, -0.04263, 0.51632), \quad E_4 = (0, 0, 0.99001),$$

$$E_5 = (0, 0.99001, 0), \quad E_6 = (0.46786, 0.03929, 0.47286), \quad E_7 = (0.9, 0, -1.16018^{-16}), \quad E_8 = (0.9, 0, 0).$$

The eigenvalues of the matrix of E_1 are $\lambda_{11} = (11.979, 0.999, -0.99)$, E_2 is $\lambda_{12} = (0.99, 0.99, 0.09)$, E_3 is $\lambda_{13} = (0.136895, 0.0426316, -0.0426316)$, E_4 is $\lambda_{14} = (-0.99, -0.99, 0.09)$, E_5 is $\lambda_{15} = (-0.999, -0.99, 0.99)$, E_6 is $\lambda_{16} = (-0.551065, -0.000181701 \pm 0.198837i)$, E_7 is $\lambda_{17} = (0.99, -0.09, 6.93889 \times 10^{-17})$ and E_8 is $\lambda_{18} = (0.99, -0.09, -2.77556 \times 10^{-17})$. Clearly, by using the condition $|arg(\lambda)|$ all the equilibrium points are unstable for all orders α of the Caputo derivative.

5. Existence and uniqueness of the solutions

The Banach fixed-point theorem is used in this section to prove the existence and distinctiveness of the solutions to the suggested model. Due to the complexity and non-local behavior of the model (2), there are no direct methods for evaluating the precise solutions; nonetheless, if certain requirements are met, the solution's existence can be guaranteed. Then by (2), we have

$$\begin{aligned} D_t^{\rho}[P_A(t)] &= \mathcal{G}_1(t, P_A), \\ D_t^{\rho}[P_B(t)] &= \mathcal{G}_2(t, P_B), \\ D_t^{\rho}[P_C(t)] &= \mathcal{G}_3(t, P_C). \end{aligned} \tag{11}$$

With a Volterra-type integral equation, we have

$$\begin{aligned} P_A(t) - P_A(t_0) &= \frac{1}{\Gamma(\rho)} \int_{t_0}^{t} \mathcal{G}_1(\vartheta, P_A)(t - \vartheta)^{\rho - 1} d\vartheta, \\ P_B(t) - P_B(t_0) &= \frac{1}{\Gamma(\rho)} \int_{t_0}^{t} \mathcal{G}_2(\vartheta, P_B)(t - \vartheta)^{\rho - 1} d\vartheta, \\ P_C(t) - P_C(t_0) &= \frac{1}{\Gamma(\rho)} \int_{t_0}^{t} \mathcal{G}_3(\vartheta, P_C)(t - \vartheta)^{\rho - 1} d\vartheta. \end{aligned} \tag{12}$$

Theorem 5.1. *The kernel $\mathcal{G}_1$ holds the Lipschitz condition and contraction if $0 \leq (\alpha_1(1 - (\nu_1 + \nu_1^{'}) - \nu_2 - \nu_3) + \Omega_3\nu_3 - \Omega_1\nu_2 - \beta) < 1$ holds.*

Proof. We shall consider the two functions P_A and P_{A1} such as:

$$\begin{aligned} \|\mathcal{G}_1(t, P_A) - \mathcal{G}_1(t, P_{A1})\| &= \| P_A[\alpha_1(1 - P_A - P_B - P_C) + \Omega_3 P_C - \Omega_1 P_B - \beta] \\ &\quad - (P_{A1}[\alpha_1(1 - P_{A1} - P_B - P_C) + \Omega_3 P_C - \Omega_1 P_B - \beta]) \| \\ &\leq \|(\alpha_1(1 - (P_A + P_{A1}) - P_B - P_C) + \Omega_3 P_C - \Omega_1 P_B - \beta)\| \, \|P_A(t) - P_A(t_1)\| \\ &\leq (\alpha_1(1 - (\nu_1 + \nu_1^{'}) - \nu_2 - \nu_3) + \Omega_3\nu_3 - \Omega_1\nu_2 - \beta) \, \|P_A(t) - P_A(t_1)\| \\ &\leq \zeta_1 \|P_A(t) - P_A(t_1)\|, \end{aligned} \tag{13}$$

where $\|P_A\| \leq \nu_1$, $\|P_B\| \leq \nu_2$, and $\|P_C\| \leq \nu_3$. Taking $\zeta_1 = \alpha_1(1 - (\nu_1 + \nu_1^{'}) - \nu_2 - \nu_3) + \Omega_3\nu_3 - \Omega_1\nu_2 - \beta$, we have

$$\|\mathcal{G}_1(t, P_A) - \mathcal{G}_1(t, P_{A1})\| \leq \zeta_1 \|P_A - P_A(t_1)\|. \tag{14}$$

Therefore, $\mathcal{G}_1$ satisfies the Lipschitz condition, and if $0 \leq (\alpha_1(1-(\nu_1+\nu_1^{'})-\nu_2-\nu_3)+\Omega_3\nu_3-\Omega_1\nu_2-\beta) < 1$, then it follows a contraction. Similarly, for the remaining cases, it can be proved and represented as follows

$$\begin{aligned} &\|\mathcal{G}_2(t, P_B) - \mathcal{G}_2(t, P_{B1})\| \leq \zeta_2 \|P_B(t) - P_B(t_1)\|, \\ &\|\mathcal{G}_3(t, P_C) - \mathcal{G}_3(t, P_{C1})\| \leq \zeta_3 \|P_C(t) - P_C(t_1)\|. \end{aligned} \tag{15}$$

Now, by system (12), the recursive form is

$$\begin{aligned} P_{An}(t) &= P_{A0}(t) + \frac{1}{\Gamma(\rho)} \int_{t_0}^{t} \mathcal{G}_1(\vartheta, P_{An-1})(t-\vartheta)^{\rho-1} d\vartheta, \\ P_{Bn}(t) &= P_{B0}(t) + \frac{1}{\Gamma(\rho)} \int_{t_0}^{t} \mathcal{G}_2(\vartheta, P_{Bn-1})(t-\vartheta)^{\rho-1} d\vartheta, \\ P_{Cn}(t) &= P_{C0}(t) + \frac{1}{\Gamma(\rho)} \int_{t_0}^{t} \mathcal{G}_3(\vartheta, P_{Cn-1})(t-\vartheta)^{\rho-1} d\vartheta, \end{aligned} \tag{16}$$

with

$$P_{A0}(t) = P_A(t_0),\ P_{B0}(t) = P_B(t_0),\ P_{C0}(t) = P_C(t_0).$$

Then by the successive terms difference, we have

$$\begin{aligned} \aleph_{1,n}(t) &= P_{An}(t) - P_{An-1}(t) = \frac{1}{\Gamma(\rho)} \int_{t_0}^{t} (\mathcal{G}_1(\vartheta, P_{An-1}) - \mathcal{G}_1(\vartheta, P_{An-2}))(t-\vartheta)^{\rho-1} d\vartheta, \\ \aleph_{2,n}(t) &= P_{Bn}(t) - P_{Bn-1}(t) = \frac{1}{\Gamma(\rho)} \int_{t_0}^{t} (\mathcal{G}_2(\vartheta, P_{Bn-1}) - \mathcal{G}_2(\vartheta, P_{Bn-2}))(t-\vartheta)^{\rho-1} d\vartheta, \\ \aleph_{3,n}(t) &= P_{Cn}(t) - P_{Cn-1}(t) = \frac{1}{\Gamma(\rho)} \int_{t_0}^{t} (\mathcal{G}_3(\vartheta, P_{Cn-1}) - \mathcal{G}_3(\vartheta, P_{Cn-2}))(t-\vartheta)^{\rho-1} d\vartheta. \end{aligned} \tag{17}$$

Notice that,

$$\begin{aligned} P_{An}(t) &= \sum_{i=1}^{n} \aleph_{1,i}(t), \\ P_{Bn}(t) &= \sum_{i=1}^{n} \aleph_{2,i}(t), \\ P_{Cn}(t) &= \sum_{i=1}^{n} \aleph_{3,i}(t). \end{aligned}$$

Applying norm on system (17) and then using Eq. (14), we have

$$\begin{aligned} \|\aleph_{1,n}(t)\| &\leq \frac{1}{\Gamma(\rho)} \zeta_1 \int_{t_0}^{t} \|\aleph_{1,n-1}(\vartheta)\| d\vartheta, \\ \|\aleph_{2,n}(t)\| &\leq \frac{1}{\Gamma(\rho)} \zeta_2 \int_{t_0}^{t} \|\aleph_{2,n-1}(\vartheta)\| d\vartheta, \\ \|\aleph_{3,n}(t)\| &\leq \frac{1}{\Gamma(\rho)} \zeta_3 \int_{t_0}^{t} \|\aleph_{3,n-1}(\vartheta)\| d\vartheta. \end{aligned} \tag{18}$$

By using the above theorem, we prove the following results.

Theorem 5.2. *The solution of the system of fractional differential equations (2) will exist and is unique if we obtain some t_0 such that*

$$\frac{1}{\Gamma(\rho)} \zeta_i t_0 < 1, \text{ for } i = 1, 2, 3.$$

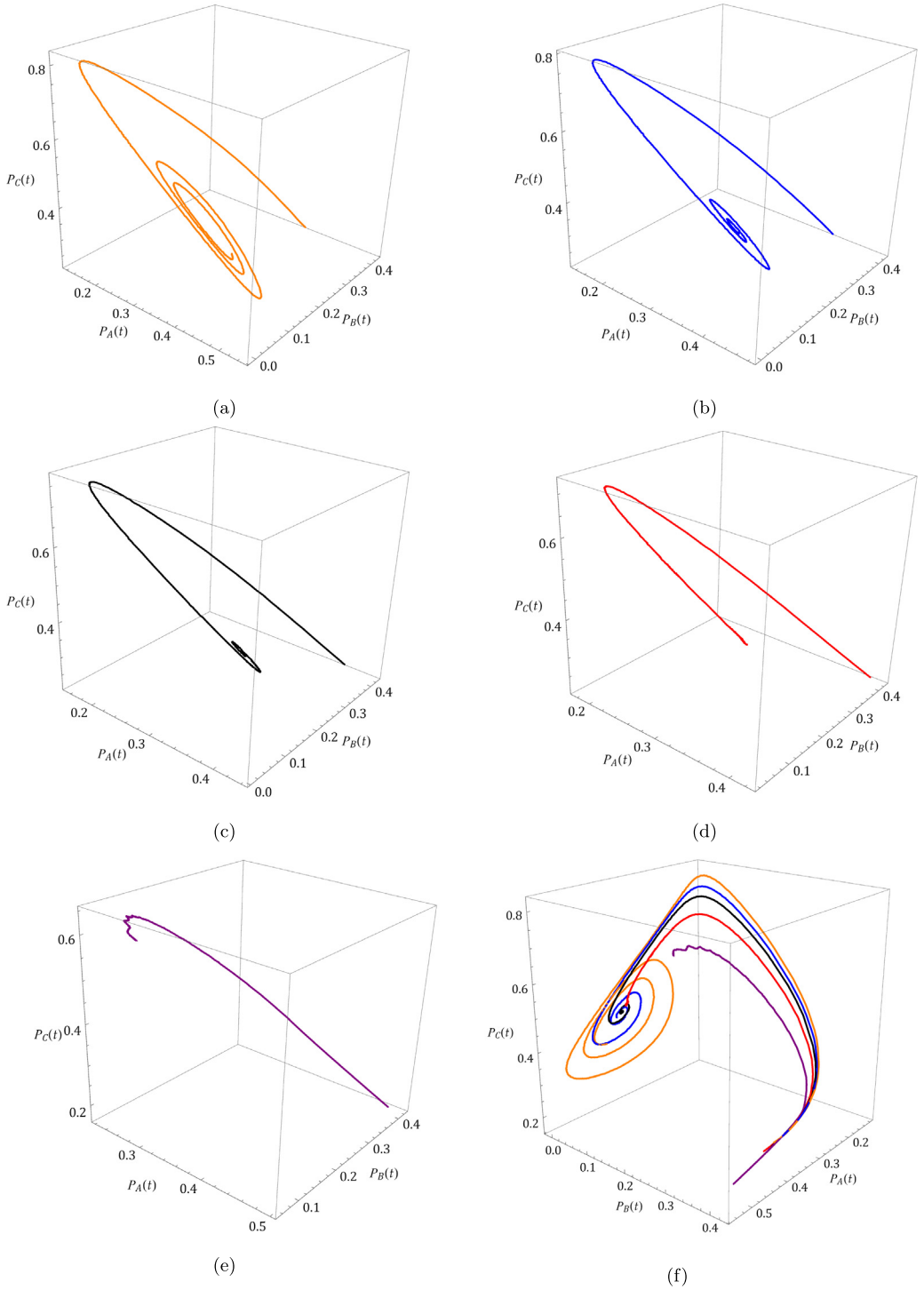

Fig. 1. 3D parametric plots for ρ are (*a*) 1, (*b*) 0.95, (*c*) 0.9, (*d*) 0.8, (*e*) 0.5 and (*e*) combined with $\alpha_1 = 0.1, \alpha_2 = 1, \alpha_3 = 1, \beta = 0.01$, $\Omega_1 = 1$, $\Omega_2 = 1$ and $\Omega_3 = 0.1$.

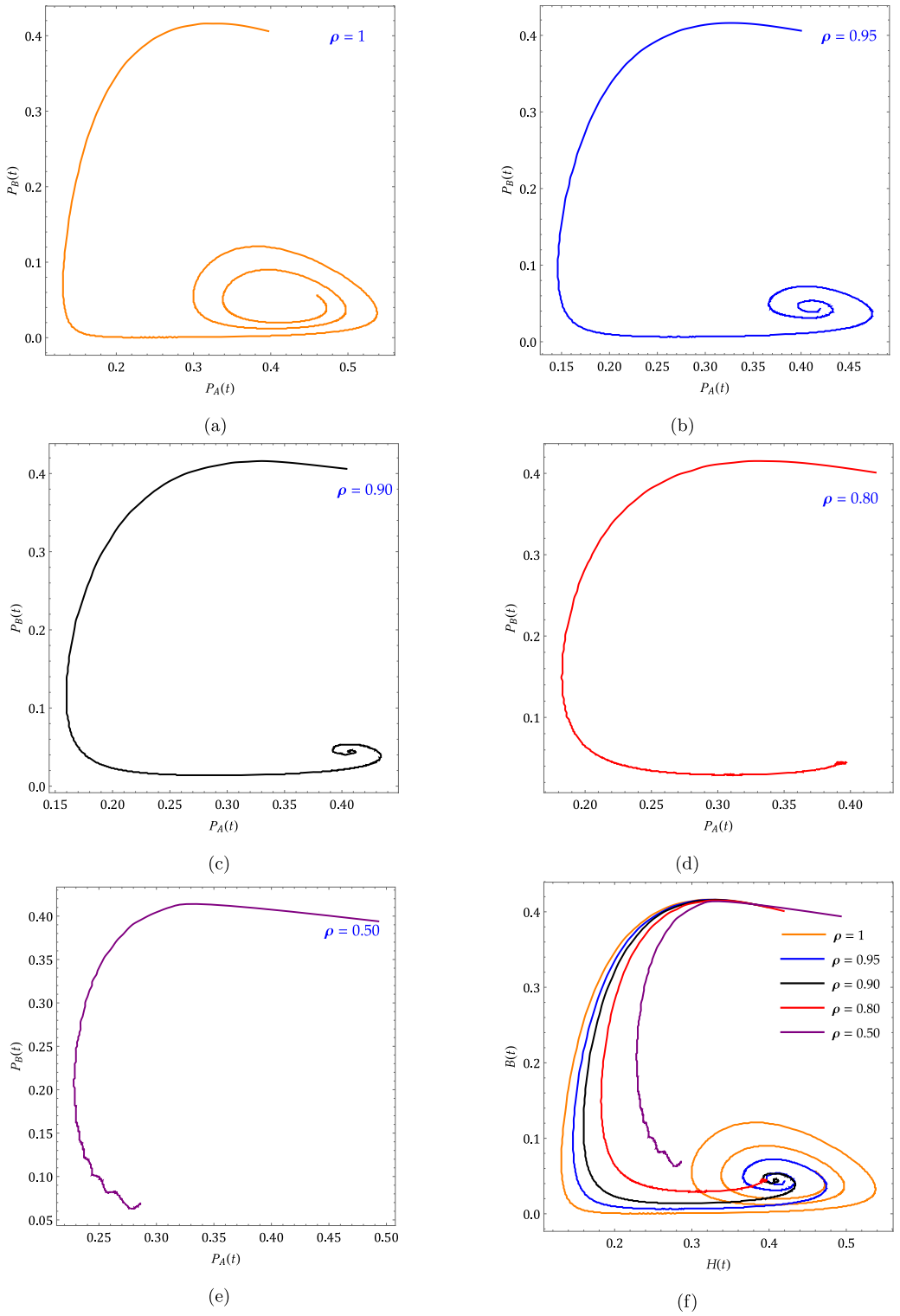

Fig. 2. 2D parametric plots for P_A v/s P_B at ρ are (*a*) 1, (*b*) 0.95, (*c*) 0.9, (*d*) 0.8, (*e*) 0.5 and (*e*) with $\alpha_1 = 0.1, \alpha_2 = 1, \alpha_3 = 1, \beta = 0.01, \Omega_1 = 1, \Omega_2 = 1$ and $\Omega_3 = 0.1$.

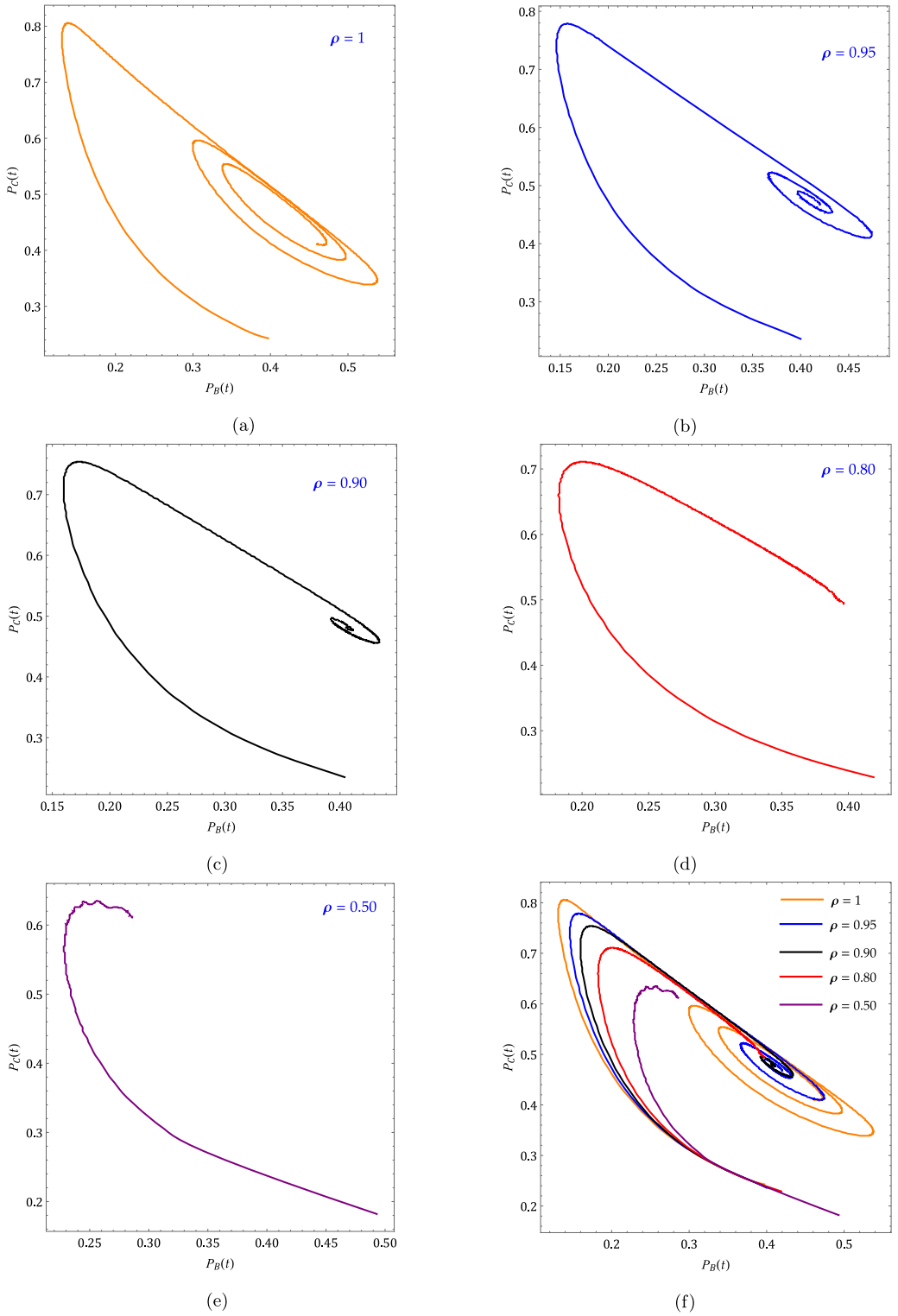

Fig. 3. 2D parametric plots for P_B v/s P_C at ρ are (*a*) 1, (*b*) 0.95, (*c*) 0.9, (*d*) 0.8, (*e*) 0.5 and (*e*) combined with $\alpha_1 = 0.1, \alpha_2 = 1, \alpha_3 = 1, \beta = 0.01, \Omega_1 = 1, \Omega_2 = 1$ and $\Omega_3 = 0.1$.

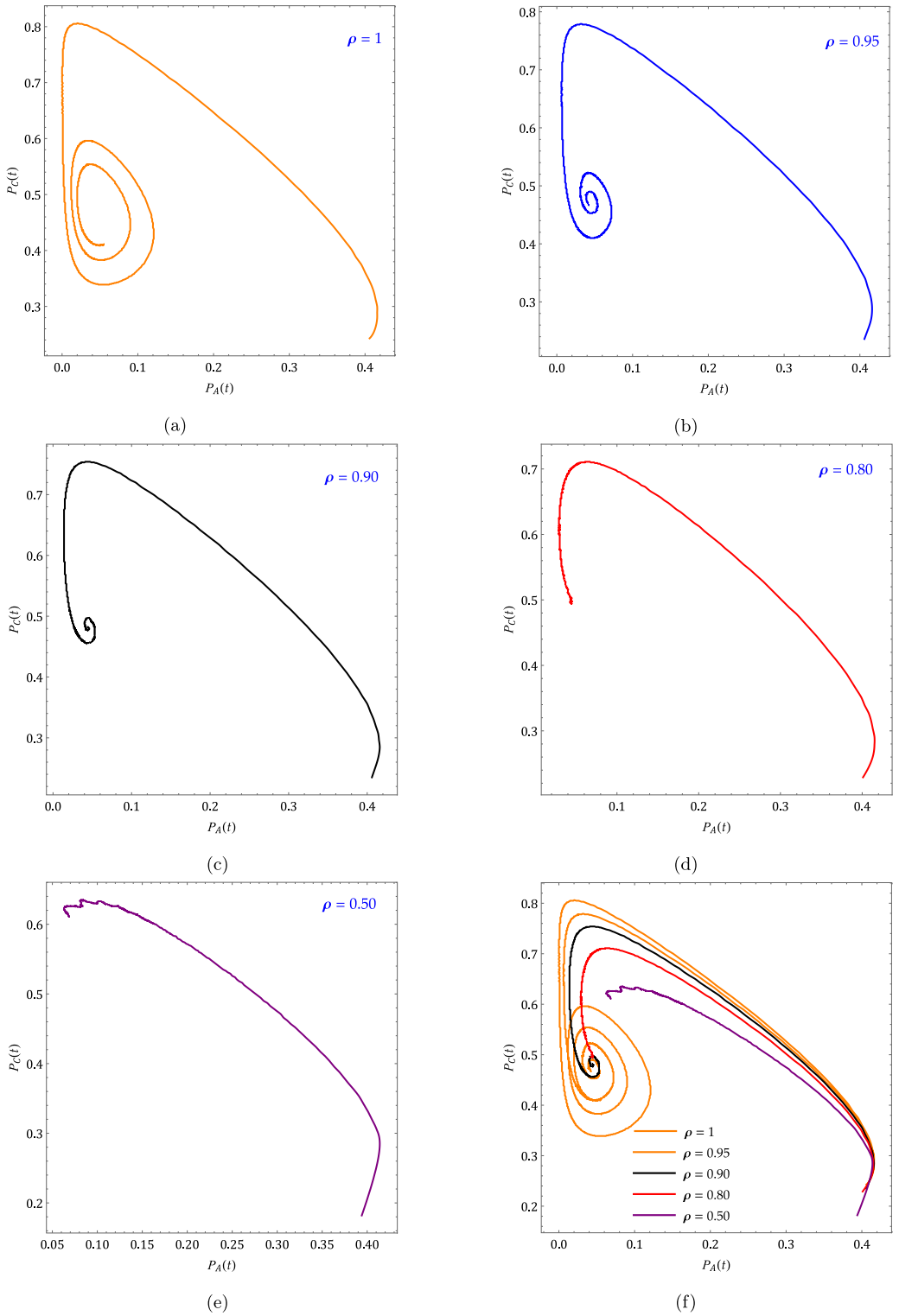

Fig. 4. 2D parametric plots for P_A v/s P_C at ρ are (*a*) 1, (*b*) 0.95, (*c*) 0.9, (*d*) 0.8, (*e*) 0.5 and (*e*) combined with $\alpha_1 = 0.1, \alpha_2 = 1, \alpha_3 = 1, \beta = 0.01, \Omega_1 = 1, \Omega_2 = 1$ and $\Omega_3 = 0.1$.

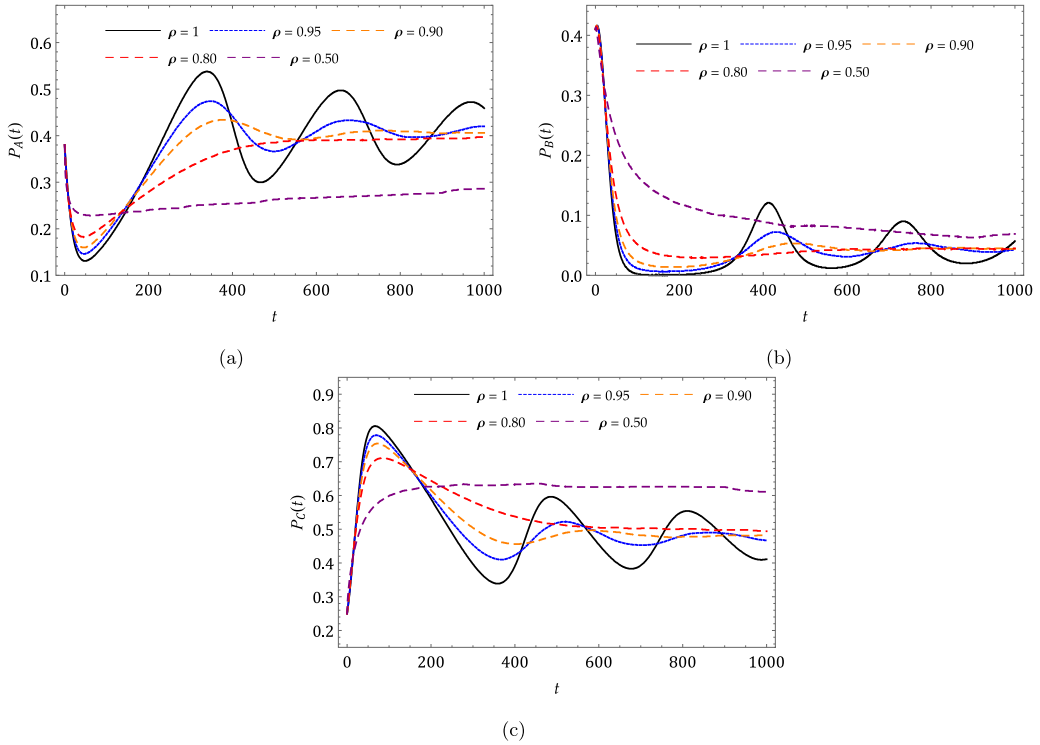

Fig. 5. Time series graph for (*a*) P_A, (*b*) P_B and P_C at $\alpha_1 = 0.1, \alpha_2 = 1, \alpha_3 = 1, \beta = 0.01, \Omega_1 = 1, \Omega_2 = 1$ and $\Omega_3 = 0.1$.

Proof. Let $P_A(t)$, $P_B(t)$ and $P_C(t)$ be the bounded functions which satisfy the Lipschitz condition. Now, by Eq. (18), we have

$$\begin{aligned}
\|\aleph_{1,i}(t)\| &\leq \|P_{An}(t_0)\| \left[\frac{1}{\Gamma(\rho)}\zeta_1\right]^n, \\
\|\aleph_{2,i}(t)\| &\leq \|P_{Bn}(t_0)\| \left[\frac{1}{\Gamma(\rho)}\zeta_2\right]^n, \\
\|\aleph_{3,i}(t)\| &\leq \|P_{Cn}(t_0)\| \left[\frac{1}{\Gamma(\rho)}\zeta_3\right]^n.
\end{aligned} \tag{19}$$

Hence, both the existence and continuity are shown for the obtained solutions. To prove that the relation (19) is the solution for (2), we consider:

$$\begin{aligned}
P_A(t) - P_A(t_0) &= P_{An}(t) - \mathfrak{W}_{1n}(t), \\
P_B(t) - P_B(t_0) &= P_{Bn}(t) - \mathfrak{W}_{2n}(t), \\
P_C(t) - P_C(t_0) &= P_{Cn}(t) - \mathfrak{W}_{3n}(t).
\end{aligned}$$

Now, we set

$$\begin{aligned}
\|\mathfrak{W}_{1n}(t)\| &= \|\frac{1}{\Gamma(\rho)}\int_{t_0}^{t}(t-\vartheta)^{\rho-1}(\mathcal{G}_1(\vartheta, P_A) - \mathcal{G}_1(\vartheta, P_{An-1}))d\vartheta\| \\
&\leq \frac{1}{\Gamma(\rho)}\int_{t_0}^{t}(t-\vartheta)^{\rho-1}\|(\mathcal{G}_1(\vartheta, P_A) - \mathcal{G}_1(\vartheta, P_{An-1}))\|d\vartheta \\
&\leq \frac{1}{\Gamma(\rho)}\zeta_1\|P_A - P_{An-1}\|t.
\end{aligned} \tag{20}$$

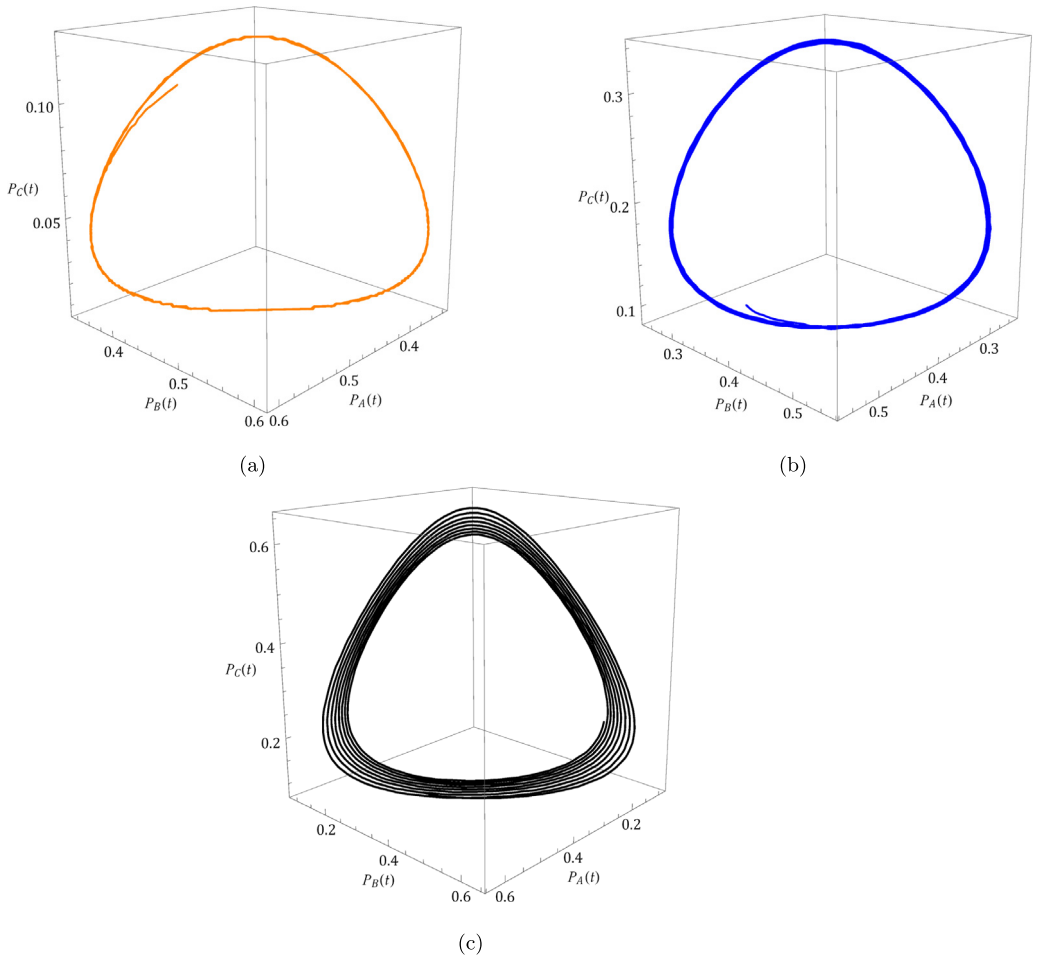

Fig. 6. 3D parametric plots for (a) $\Omega_1 = 0.1, (b)$ $\Omega_1 = 0.5$ and (c) $\Omega_1 = 1$ with $\rho = 1, \alpha_1 = 0.1, \alpha_2 = 1, \alpha_3 = 1, \beta = 0.01, \Omega_2 = 1$ and $\Omega_3 = 0.1$.

Continuing the same procedure, at t_0, we get

$$\|\mathfrak{W}_{1n}(t)\| \leq \left(\frac{t_0}{\Gamma(\rho)}\right)^{n+1} \zeta_1^{n+1} M. \tag{21}$$

From Eq. (21), we can see that as n tends to ∞, $\|\mathfrak{W}_{1n}(t)\|$ approaches to 0 provided $\frac{t_0}{\Gamma(\rho)} < 1$. Similarly, it can be proved that all $\|\mathfrak{W}_{2n}(t)\|, \|\mathfrak{W}_{3n}(t)\|$ tends to 0.

We prove uniqueness on contrary, if there exists other set of solutions $P_A^*(t), P_B^*(t), P_C^*(t)$. Then,

$$P_A(t) - P_A^*(t) = \frac{1}{\Gamma(\rho)} \int_{t_0}^{t} (\mathcal{G}_1(\vartheta, P_A) - \mathcal{G}_1(\vartheta, P_A^*)) d\vartheta.$$

By employing the norm, the above equation becomes

$$\begin{aligned} \|P_A(t) - P_A^*(t)\| &= \|\frac{1}{\Gamma(\rho)} \int_{t_0}^{t} (\mathcal{G}_1(\vartheta, P_A) - \mathcal{G}_1(\vartheta, P_A^*)) d\vartheta\| \\ &\leq \frac{1}{\Gamma(\rho)} \zeta_1 t \|P_A - P_A^*(t)\|. \end{aligned} \tag{22}$$

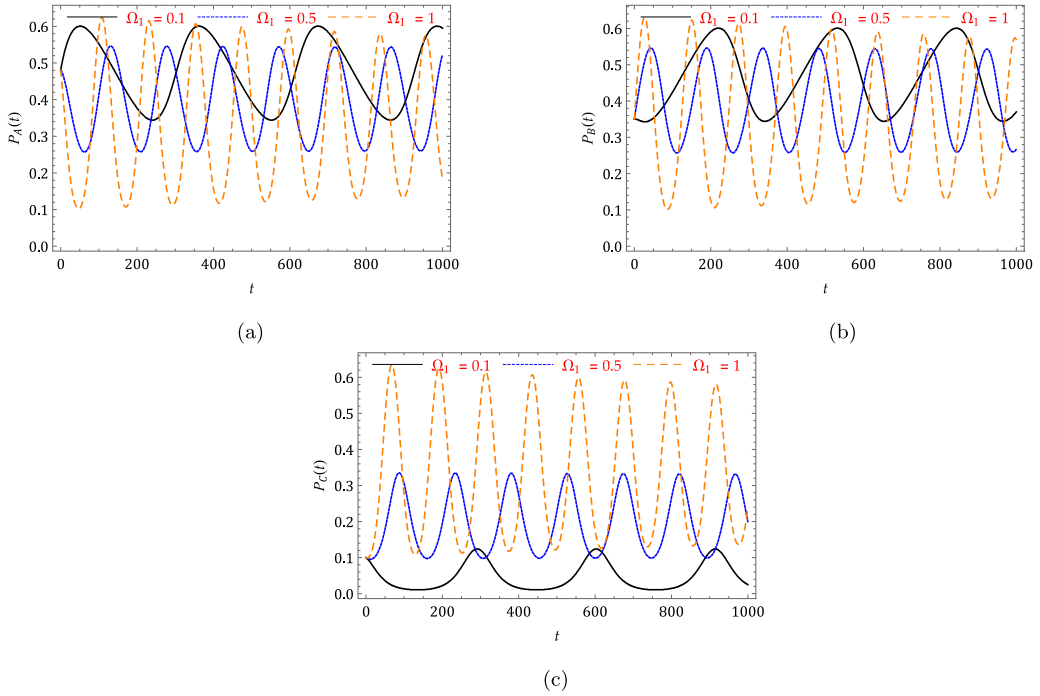

Fig. 7. Time series graph for (*a*) P_A, (*b*) P_B and (*c*) P_C at $\alpha_1 = 0.1, \alpha_2 = 1, \alpha_3 = 1, \beta = 0.01, \alpha_1 = 1, \Omega_2 = 1$ and $\Omega_3 = 0.1$ for different Ω_1.

For some t_0, one can get

$$\|P_A(t) - P_A^*(t)\|\left(1 - \frac{1}{\Gamma(\rho)}\zeta_1 t_0\right) \leq 0.$$

Since

$$\left(1 - \frac{1}{\Gamma(\rho)}\zeta_1 t\right) \geq 0, \tag{23}$$

from the above inequality, it is clear that $P_A(t) - P_A^*(t) = 0$. Hence, Eq. (23) proves the required result.

6. Numerical method

Here, employ the most cited numerical Adams–Bashforth–Moulton (ABM) method to find the solution. Now, consider

$$\begin{aligned} {}^{C}D_t^{\rho} y(t) &= \phi(t, y(t)), \quad 0 \leq t \leq T, \\ y^{(m)}(0) &= y_0^{(m)}, \quad m = 0, 1, 2, 3, \ldots, \nu, \ \nu = \lceil \rho \rceil. \end{aligned} \tag{24}$$

The Volterra integral equation of (24) is of the form

$$y(t) = \sum_{m=0}^{\nu-1} y_0^{(m)} \frac{t^m}{m!} + \frac{1}{\Gamma(\rho)} \int_0^t (t-s)^{\rho-1} \phi(s, y(s)) ds. \tag{25}$$

Diethelm and his co-authors in [21] have successfully used ABM technique by setting $h = \frac{T}{N}$, $t_n = nh$, $n = 0, 1, 2, \ldots, N \in Z^+$ to integrate Eq. (25), The system (2) in a simplified equation is

$$\begin{aligned} D_t^{\rho} P_A(t) &= P_A[\alpha_1(1 - P_A - P_B - P_C) + \Omega_3 P_C - \Omega_1 P_B - \beta], \\ D_t^{\rho} P_B(t) &= P_B[\alpha_2(1 - P_A - P_B - P_C) + \Omega_1 P_A - \Omega_2 P_C - \beta], \\ D_t^{\rho} P_C(t) &= P_C[\alpha_3(1 - P_A - P_B - P_C) + \Omega_2 P_B - \Omega_3 P_A - \beta]. \end{aligned} \tag{26}$$

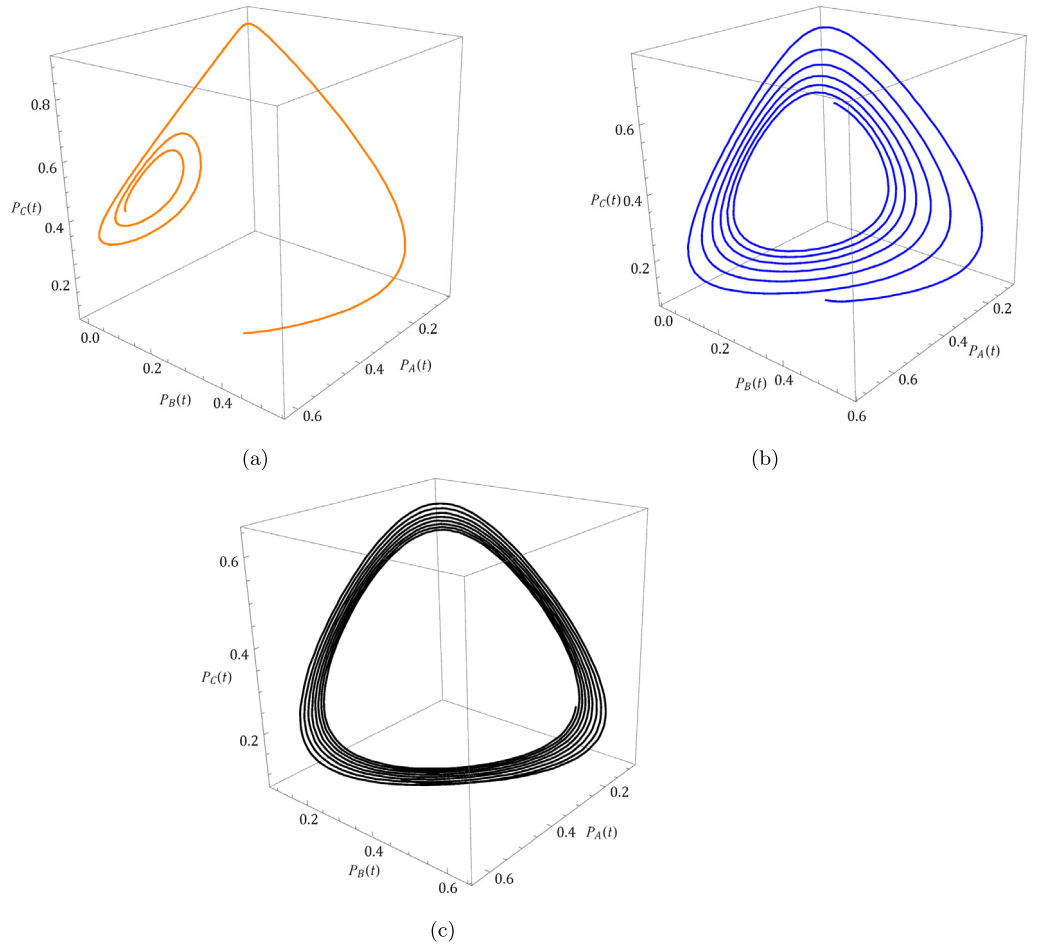

Fig. 8. 3D parametric plots for (a) $\Omega_3 = 0.1$, (b) $\Omega_3 = 0.5$ and (c) $\Omega_3 = 1$ with $\rho = 1, \alpha_1 = 0.1, \alpha_2 = 1, \alpha_3 = 1, \beta = 0.01, \Omega_1 = 1$ and $\Omega_2 = 1$.

Then

$$
\begin{aligned}
P_{An+1} &= P_{A0} + \frac{h^\rho}{\Gamma(\rho+2)}\left(P_{A_{n+1}}^H[\alpha_1(1 - P_{A_{n+1}}^H - P_{B_{n+1}}^H - P_{C_{n+1}}^H) + \Omega_3 P_{C_{n+1}}^H - \Omega_1 P_{B_{n+1}}^H - \beta]\right) \\
&\quad + \frac{h^\rho}{\Gamma(\rho+2)}\sum_{i=0}^{n} a_{i,n+1}\left(P_{Ai}[\alpha_1(1 - P_{Ai} - P_{Bi} - P_{Ci}) + \Omega_3 P_{Ci} - \Omega_1 P_{Bi} - \beta]\right), \\
P_{Bn+1} &= P_{B0} + \frac{h^\rho}{\Gamma(\rho+2)}\left(P_{B_{n+1}}^H[\alpha_2(1 - P_{A_{n+1}}^H - P_{B_{n+1}}^H - P_{C_{n+1}}^H) + \Omega_1 P_{A_{n+1}}^H - \Omega_2 P_{C_{n+1}}^H - \beta]\right) \\
&\quad + \frac{h^\rho}{\Gamma(\rho+2)}\sum_{i=0}^{n} a_{i,n+1}\left(P_{Bi}[\alpha_2(1 - P_{Ai} - P_{Bi} - P_{Ci}) + \Omega_1 P_{Ai} - \Omega_2 P_{Ci} - \beta]\right), \\
P_{Cn+1} &= P_{C0} + \frac{h^\rho}{\Gamma(\rho+2)}\left(P_{C_{n+1}}^H[\alpha_3(1 - P_{A_{n+1}}^H - P_{B_{n+1}}^H - P_{C_{n+1}}^H) + \Omega_2 P_{B_{n+1}}^H - \Omega_3 P_{A_{n+1}}^H - \beta]\right) \\
&\quad + \frac{h^\rho}{\Gamma(\rho+2)}\sum_{i=0}^{n} a_{i,n+1}\left(P_{Ci}[\alpha_3(1 - P_{Ai} - P_{Bi} - P_{Ci}) + \Omega_2 P_{Bi} - \Omega_3 P_{Ai} - \beta]\right).
\end{aligned}
\tag{27}
$$

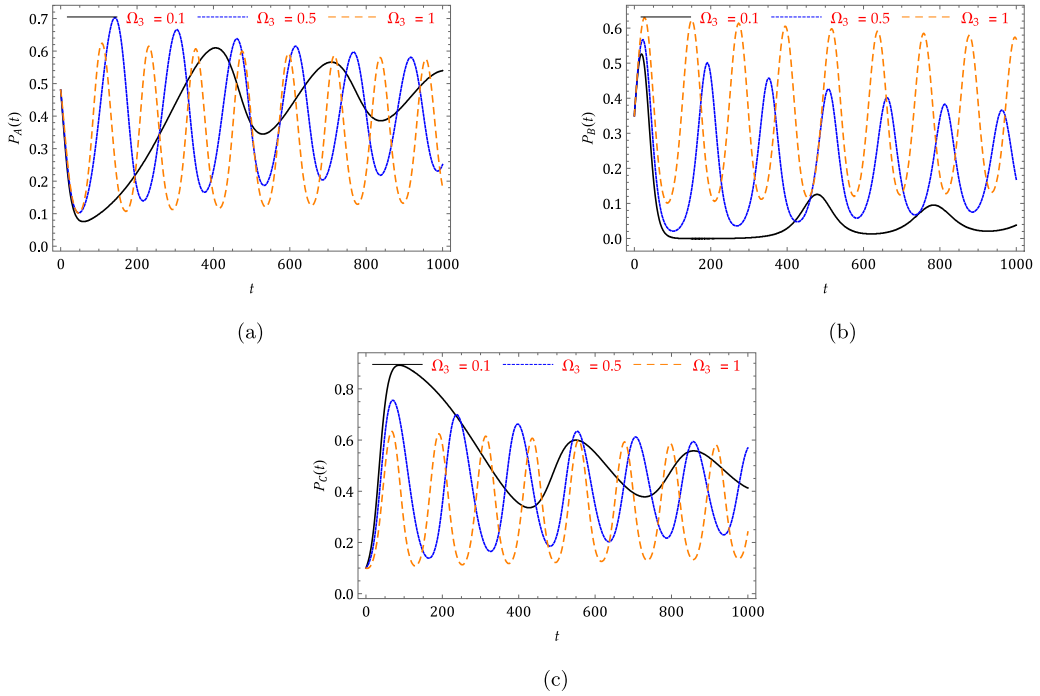

Fig. 9. Time series graph for (a) P_A, (b) P_B and $(c)P_C$ at $\alpha_1 = 0.1, \alpha_2 = 1, \alpha_3 = 1, \beta = 0.01, \alpha_1 = 1, \Omega_1 = 1$ and $\Omega_2 = 0.1$ for different Ω_3.

Here

$$
\begin{aligned}
{}^{H}_{}P_{A}{}_{n+1} &= P_{A0} + \frac{h^{\rho}}{\Gamma(\rho+1)} \sum_{i=0}^{n} b_{i,n+1} \left(P_{Ai}[\alpha_1(1 - P_{Ai} - P_{Bi} - P_{Ci}) + \Omega_3 P_{Ci} - \Omega_1 P_{Bi} - \beta] \right), \\
{}^{H}_{}P_{B}{}_{n+1} &= P_{B0} + \frac{h^{\rho}}{\Gamma(\rho+1)} \sum_{i=0}^{n} b_{i,n+1} \left(P_{Bi}[\alpha_2(1 - P_{Ai} - P_{Bi} - P_{Ci}) + \Omega_1 P_{Ai} - \Omega_2 P_{Ci} - \beta] \right), \\
{}^{H}_{}P_{C}{}_{n+1} &= P_{C0} + \frac{h^{\rho}}{\Gamma(\rho+1)} \sum_{i=0}^{n} b_{i,n+1} \left(P_{Ci}[\alpha_3(1 - P_{Ai} - P_{Bi} - P_{Ci}) + \Omega_2 P_{Bi} - \Omega_3 P_{Ai} - \beta] \right),
\end{aligned} \tag{28}
$$

$$
a_{i,n+1} = \begin{cases} n^{\rho+1} - (n-\rho)(n+1)^{\rho}, & i = 0, \\ (n-i+2)^{\rho+1} + (n-i)^{\rho+1} - 2(n-i+1)^{\rho+1}, & 1 \le i \le n, \\ 1, & i = n+1, \end{cases} \tag{29}
$$

and

$$
b_{i,n+1} = \frac{h^{\rho}}{\rho} \left((n-i+1)^{\rho} - (n-i)^{\rho} \right), \quad 0 \le i \le n. \tag{30}
$$

7. Results and discussion

The investigation of daily life activity can help us to understand the impotence and essence of investigating phenomena using mathematical theories and mathematical tools. Particularly, for the computation and graphical illustration, we used MATHEMATICA software. Here, we investigate about the dynamics of the voters with three different political parties with many assumptions. The numerical behavior of the system with a different order in

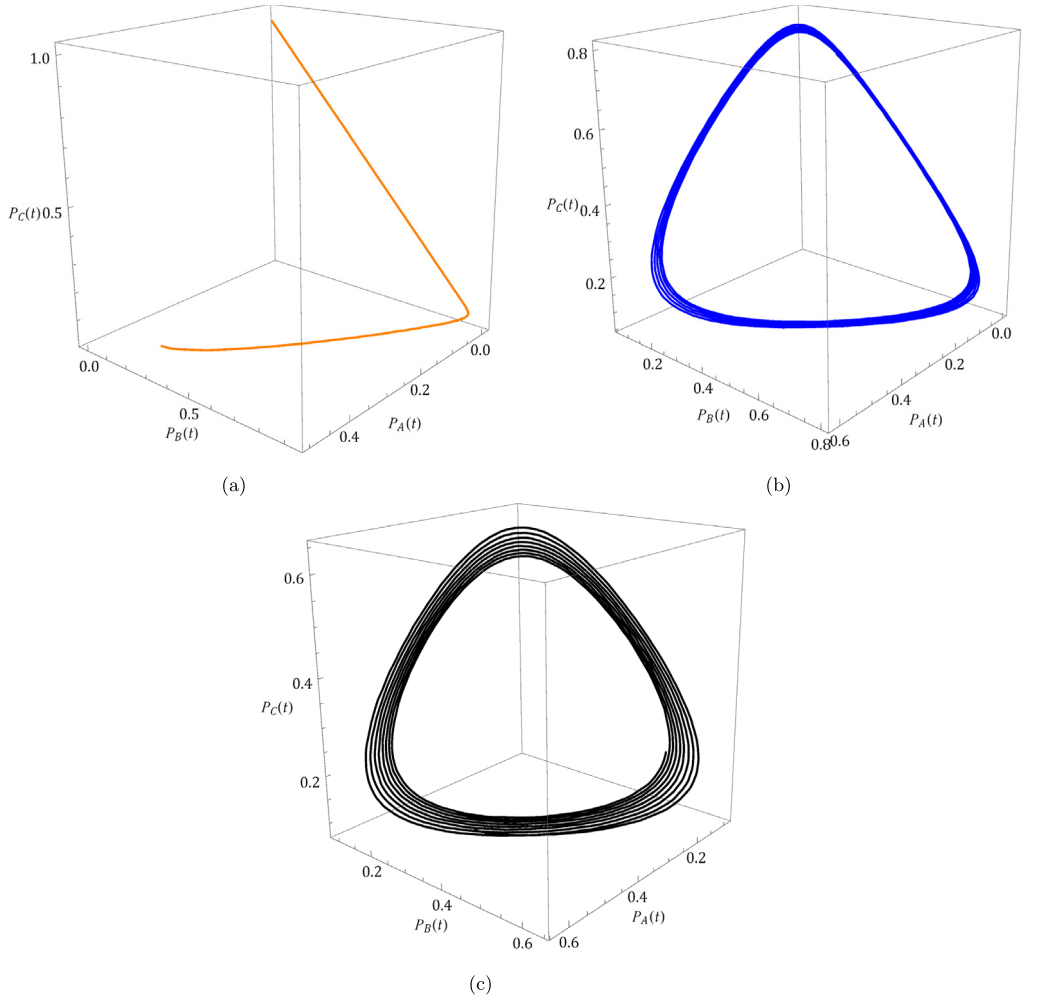

Fig. 10. 3D parametric plots for (a) $\Omega_2 = 0.1$, (b) $\Omega_2 = 0.5$ and (c) $\Omega_2 = 1$ with $\rho = 1, \alpha_1 = 0.1, \alpha_2 = 1, \alpha_3 = 1, \beta = 0.01, \Omega_1 = 1$ and $\Omega_3 = 1$.

terms of 3D-parametric plots are shown in Fig. 1. We can observe that from this figure, the changes in fractional order are simplified from unstable to being stable. In Figs. 2, we captured the changes of order in 2D parametric plots with two political parties P_A v/s P_B. In the same manner, Fig. 3 helps us to understand the interaction b/w two parties P_B v/s P_C. These figures show that as order decreases from 1 to 0.50, the spirals are reduced. It gives some idea about to stable the voters dynamics. The similar thought for P_C v/s P_A can be noticed in Fig. 4. We noticed the impact of generalizing the classical model and it helped us to understand that the density of voter transmission decreased over the periods. This can be noticed in Fig. 5.

The parameters which signify the dynamics of the voters and three political parties need huge scientific analysis because they help the policymakers and leaders of the parties to ensure stability to retain their position in the long run. In this connection, the net shift between parties is captured in Figs. 6 and 7. Specifically, the new range changes are associated with the hereditary properties of the voters who think of moving between three parties. This can be drawn in Figs. 8 and 9. If the difference between the per capita recruitment rate of P_B from party P_A and P_A from party P_B is less than the flexion of the voter as days move is less for P_A and P_B, but it will hugely affect for P_C Ω_1. In the same manner, the recruitment rate of P_C from party P_B and P_B from party P_C, and the recruitment rate of P_A from party P_C and P_C from party P_A have a significant impact on the three parties and corresponding supporters (Figs. 10 and 11).

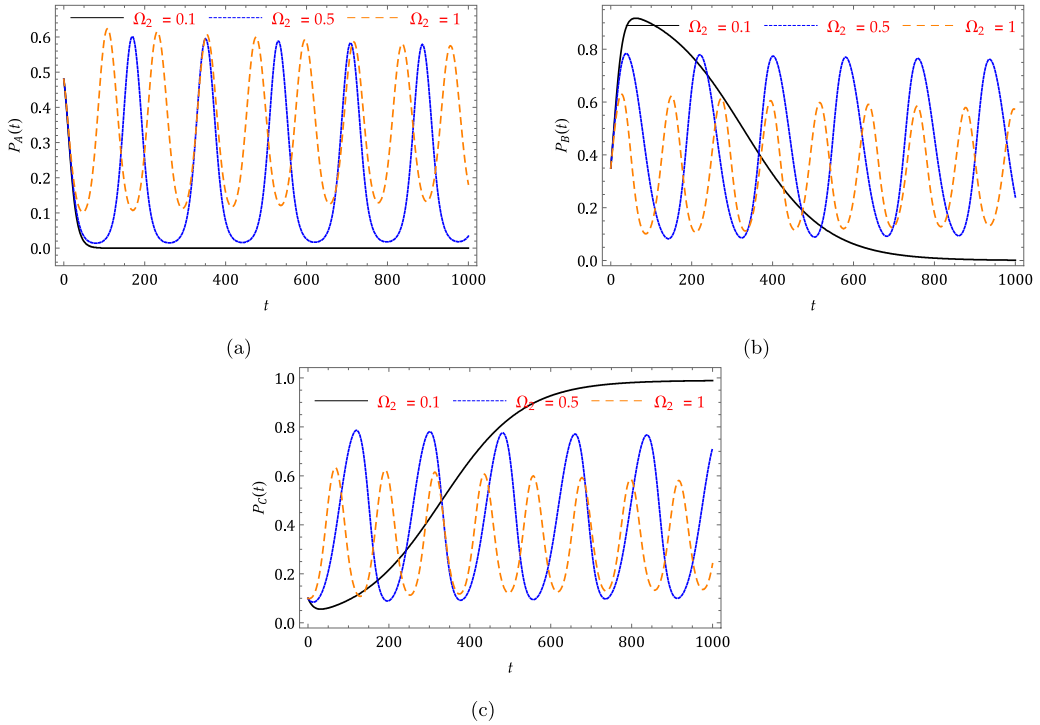

Fig. 11. Time series graph for (*a*) P_A, (*b*) P_B and (*c*) P_C at $\alpha_1 = 0.1, \alpha_2 = 1, \alpha_3 = 1, \beta = 0.01, \alpha_1 = 1, \Omega_1 = 1$ and $\Omega_3 = 1$ for different Ω_2.

8. Conclusion

The primary finding of the current study illustrates the impact of the fractional operator on the three-party political system. Because of the projected model's instability, which was discovered during the current inquiry, we can see how intricate it is. We can select the parameter to regulate the political system with the aid of the depicted dynamical analysis. The parameter Ω_i $(i = 1, 2, 3)$ signifies the net shift between party and plays an vital role in the present investigation as well as dynamics of the projected system. In order to illustrate the its effect on dynamics, we draw many figures to exact how it effects and helps political parties control the transmission from one parties to other without much concerning about other parties. We were able to achieve the results with the use of a tried-and-true numerical method, and we then conducted more research using various values of the parameters. The capacity of the fractional operator to get the behavior related with the complexity of the three parties can be confirmed with the aid of the stated graphical findings. Conclusively, we emphasize the importance of generalizing the integer order model in order to capture its fundamental behavior and forecast the relevant effects of the voters with three political parties using appropriate assumptions and parameter selection. This research opens the way to comprehending the fractional order deeper meaning when looking at happenings in the real world.

References

[1] B.S.T. Alkahtani, A. Atangana, I. Koca, Novel analysis of the fractional Zika model using the Adams type predictor–corrector rule for non-singular and non-local fractional operators, J. Nonlinear Sci. Appl. 10 (6) (2017) 3191–3200.
[2] M.P. Anilkumar, K.P. Jose, Analysis of a discrete time queueing-inventory model with back-order of items, 3c Empresa: Investigación Y Pensamiento CríTico 11 (2) (2022) 50–62.
[3] A. Atangana, D. Baleanu, New fractional derivatives with non-local and non-singular kernel theory and application to heat transfer model, Therm. Sci. 20 (2016) 763–769.
[4] C. Baishya, P. Veeresha, Laguerre polynomial-based operational matrix of integration for solving fractional differential equations with non-singular kernel, Proc. Roy. Soc. A 477 (2253) (2021).
[5] O. Balatif, A. Labzai, M. Rachik, A discrete mathematical modeling and optimal control of the electoral behavior with regard to a political party, Discrete Dyn. Nat. Soc. 2018 (2018) 1–14.

[6] D. Baleanu, F. Akhavan Ghassabzade, J.J. Nieto, A. Jajarmi, On a new and generalized fractional model for a real cholera outbreak, Alex. Eng. J. 61 (11) (2022) 9175–9186.
[7] D. Baleanu, Z.B. Guvenc, J.A. Tenreiro Machado, New Trends in Nanotechnology and Fractional Calculus Applications, Springer Dordrecht Heidelberg, London New York, 2010.
[8] D. Baleanu, A. Jajarmi, H. Mohammadi, S. Rezapour, A new study on the mathematical modelling of human liver with Caputo–Fabrizio fractional derivative, Chaos Solitons Fractals 134 (2020) 109705.
[9] S. Banuelos, T. Danet, C. Flores, A. Ramos, An epidemiological math model approach to a political system with three parties, CODEE J. 12 (1) (2019) 8.
[10] L. Beghin, M. Caputo, Commutative and associative properties of the Caputo fractional derivative and its generalizing convolution operator, Commun. Nonlinear Sci. Numer. Simul. 89 (2020) 105338.
[11] A.S. Belenky, D.C. King, A mathematical model for estimating the potential margin of state undecided voters for a candidate in a US federal election, Math. Comput. Modelling 45 (2007) 585–593.
[12] D.V. Bhise, S.A. Choudhari, M.A. Kumbhalkar, M.M. Sardeshmukh, Modelling the critical success factors for advanced manufacturing technology implementation in small and medium sized enterprises, 3c Empresa: Investigacion Y Pensamiento CríTico 11 (2) (2022) 263–275.
[13] Dattatraya V. Bhise, Sumant A. Choudhari, Manoj A. Kumbhalkar, Mhalsakant M. Sardeshmukh, Modelling the critical success factors for advanced manufacturing technology implementation in small and medium sized enterprises, 3c Empresa: Investigación Y Pensamiento CríTico 11 (2) (2022) 263–275.
[14] K. Calderon, C. Orbe, A. Panjwani, D.M. Romero, C. Kribs-Zaleta, K. Ríos-Soto, An epidemiological approach to the spread of political third parties, mtbi.asu.edu/Summer-2005.html.
[15] M. Caputo, Linear models of dissipation whose Q is almost frequency independent-II, Geophys. J. Int. 13 (5) (1967) 529–539.
[16] M. Caputo, Elasticita e dissipazione, 1969, Zanichelli, Bologna.
[17] M. Caputo, M. Fabrizio, A new definition of fractional derivative without singular kernel, Prog. Fract. Differ. Appl. 1 (2) (2015) 73–85.
[18] O. Defterli, D. Baleanu, A. Jajarmi, S.S. Sajjadi, N. Alshaikh, J.H. Asad, Fractional treatment: An accelerated mass–spring system, Rom. Rep. Phys. 74 (4) (2022) 122.
[19] K. Diethelm, An algorithm for the numerical solution of differential equations of fractional order, Electron. Trans. Numer. Anal. 5 (1) (1997) 1–6.
[20] K. Diethelm, N.J. Ford, Analysis of fractional differential equations, J. Math. Anal. Appl. 265 (2) (2002) 229–248.
[21] K. Diethelm, N.J. Ford, A.D. Freed, A predictor–corrector approach for the numerical solution of fractional differential equations, Nonlinear Dynam. 29 (1) (2002) 3–22.
[22] E. Fieldhouse, N. Shryane, A. Pickles, Strategic voting and constituency context: Modelling party preference and vote in multiparty elections, Polit. Geogr. 26 (2007) 159–178.
[23] W. Gao, P. Veeresha, C. Cattani, C. Baishya, H.M. Baskonus, Modified predictor–corrector method for the numerical solution of a fractional-order SIR model with 2019-nCoV, Fractal Fractional 6 (2) (2022) 92.
[24] R. Huckfeldt, C.W. Kohfeld, Electoral stability and the decline of class in democratic politics, Math. Comput. Modelling 16 (8–9) (1992) 223–239.
[25] A. Jajarmi, D. Baleanu, S.S. Sajjadi, J.J. Nieto, Analysis and some applications of a regularized Ψ-Hilfer fractional derivative, J. Comput. Appl. Math. 415 (2022) 114476.
[26] Q.J.A. Khan, Hopf bifurcation in multiparty political systems with time delay in switching, Appl. Math. Lett. 13 (2000) 43–52.
[27] A.A. Kilbas, H.M. Srivastava, J.J. Trujillo, Theory and Applications of Fractional Differential Equations, Elsevier, Amsterdam, 2006.
[28] C. Li, C. Tao, On the fractional adams method, Comput. Math. Appl. 58 (8) (2009) 1573–1588.
[29] H.-L. Li, L. Zhang, C. Hu, Y.-L. Jiang, Z. Teng, Dynamical analysis of a fractional-order predator- prey model incorporating a prey refuge, J. Appl. Math. Comput. 54 (1) (2017) 435–449.
[30] J. Liouville, Memoire surquelques questions de geometrieet de mecanique, Et sur Un Nouveau Genre de Calcul Pour Resoudreces Questions, J. Ecole. Polytech. 13 (1832) 1–69.
[31] J. Lu, L. Zhu, W. Gao, Remarks on bipolar cubic fuzzy graphs and its chemical applications, Int. J. Math. Comput. Eng. 1 (1) (2023) 1–9.
[32] M. Luo, B. Fakieh, H. Hasan, Children's cognitive function and mental health based on finite element nonlinear mathematical model, Appl. Math. Nonlinear Sci. 7 (2) (2021) 59–68.
[33] P.S. Macansantos, Modeling dynamics of political parties with poaching from one party, J. Phys.: Conf. Ser. 1593 (1) (2020).
[34] A. Mahmud, T. Tanriverdi, K. Muhamad, Exact traveling wave solutions for (2+1)-dimensional Konopelchenko-Dubrovsky equation by using the hyperbolic trigonometric functions methods, Int. J. Math. Comput. Eng. 1 (1) (2023) 1–14, http://dx.doi.org/10.2478/ijmce-(2023)2023-0002.
[35] M. Martcheva, An Introduction to Mathematical Epidemiology,Vol. 61, Springer, 2015.
[36] D. Matignon, Stability results for fractional differential equations with applications to control processing, in: In Computational Engineering in Systems Applications, Vol. 2, Citeseer, 1996, pp. 963–968.
[37] K.S. Miller, B. Ross, An Introduction to Fractional Calculus and Fractional Differential Equations, A Wiley, New York, 1993.
[38] A.K. Misra, A simple mathematical model for the spread of two political parties, Nonlinear Anal. Model. Control 17 (2012) 343–354.
[39] F. Nyabadza, T.Y. Alassey, G. Muchatibaya, Modelling the dynamics of two political parties in the presence of switching, SpringerPlus 5 (2016) 1–11.
[40] I. Petersen, Stability of equilibria in multi-party political system, Math. Soc. Sci. 21 (1991) 81–93.
[41] I. Podlubny, Fractional Differential Equations, Academic Press, New York, 1999.

[42] I. Podlubny, Fractional Differential Equations, Academic Press, San Diego, 1999.
[43] L. Qian, S. Wei, Y. Tianlai, W. Tiancheng, H. Mohamed, Mathematical methodology in the seismic resilience evaluation of the water supply system, Appl. Math. Nonlinear Sci. (2023).
[44] V. Raghavendra, P. Veeresha, Analysing the market for digital payments in India using the predator–prey mode, Int. J. Optim. Control: Theories Appl. (IJOCTA) 13 (1) (2023) 104–115.
[45] G.F.B. Riemann, Versuch Einer Allgemeinen Auffassung der Integration und Differentiation, Gesammelte Mathematische Werke, Leipzig, 1896.
[46] N. Sene, Study of a fractional-order chaotic system represented by the Caputo operator, Complexity (2021) 1–20.
[47] Y. Valentin, G. Fail, U. Pavel, Shapley values to explain machine learning models of school student's academic performance during Covid-19, 3C TIC 11 (2) (2022) 136–144.
[48] P. Veeresha, The efficient fractional order based approach to analyze chemical reaction associated with pattern formation, Chaos Solitons Fractals 165 (2022) 112862.
[49] P. Veeresha, D. Baleanu, A unifying computational framework for fractional Gross–Pitaevskii equations, Phys. Scr. 96 (12) (2021) 125010.
[50] P. Veeresha, H.M. Baskonus, W. Gao, Strong interacting internal waves in rotating ocean: Novel fractional approach, Axioms 10 (2) (2021) 123.
[51] P. Veeresha, M. Yavuz, C. Baishya, A computational approach for shallow water forced Korteweg–De Vries equation on critical flow over a hole with three fractional operators, Int. J. Optim. Control: Theories Appl. (IJOCTA) 11 (3) (2021) 52–67.
[52] B. Wang, L.-Q. Chen, Asymptotic stability analysis with numerical confirmation of an axially accelerating beam constituted by the standard linear solid model, J. Sound Vib. 328 (4–5) (2009) 456–466.
[53] S.W. Yao, E. Ilhan, P. Veeresha, H.M. Baskonus, A powerful iterative approach for quintic complex Ginzburg–Landau equation within the frame of fractional operator, Fractals 29 (05) (2021) 2140023.